JACS
JOURNAL OF THE AMERICAN CHEMICAL SOCIETY
Communication
pubs.acs.org/JACS

Superconducting Phases in Potassium-Intercalated Iron Selenides

Tianping Ying, Xiaolong Chen,* Gang Wang,* Shifeng Jin, Xiaofang Lai, Tingting Zhou, Han Zhang, Shijie Shen, and Wanyan Wang

Research & Development Center for Functional Crystals, Beijing National Laboratory for Condensed Matter Physics, Institute of Physics, Chinese Academy of Sciences, Beijing 100190, China

Supporting Information

ABSTRACT: The ubiquitous coexistence of majority insulating 245 phases and minority superconducting (SC) phases in $A_xFe_{2-y}Se_2$ (A = K, Cs, Rb, Tl/Rb, Tl/K) formed by high-temperature routes makes pure SC phases highly desirable for studying the intrinsic properties of this SC family. Here we report that there are at least two pure SC phases, $K_xFe_2Se_2(NH_3)_y$ ($x \approx 0.3$ and 0.6), determined mainly by potassium concentration in the K-intercalated iron selenides formed via the liquid ammonia route. $K_{0.3}Fe_2Se_2(NH_3)_{0.47}$ corresponds to the 44 K phase with lattice constant c = 15.56(1) Å and $K_{0.6}Fe_2Se_2(NH_3)_{0.37}$ to the 30 K phase with c = 14.84(1) Å. With higher potassium doping, the 44 K phase can be converted into the 30 K phase. NH_3 has little, if any, effect on superconductivity. Thus, the conclusions should apply to both $K_{0.3}Fe_2Se_2$ and $K_{0.6}Fe_2Se_2$ SC phases. $K_{0.3}Fe_2Se_2(NH_3)_{0.47}$ and $K_{0.6}Fe_2Se_2(NH_3)_{0.37}$ stand out among known superconductors as their structures are stable only at particular potassium doping levels, and hence the variation of T_c with doping is not dome-like.

Considerable progress has been made in the study of $A_xFe_{2-y}Se_2$ (A = K, Cs, Rb, Tl/Rb, Tl/K) since the discovery of superconductivity at ~30 K in $K_{0.8}Fe_2Se_2$.[1] The dominant phases in $A_xFe_{2-y}Se_2$ are now identified to be $A_2Fe_4Se_5$ (so-called 245 phases) that exhibit order−disorder structural transitions due to Fe vacancies followed by antiferromagnetic orderings with large magnetic moments up to 3.3 μ_B per iron ion at T_N = 478, 534, and 559 K for A = Cs, Rb, and K, respectively.[2] These 245 phases, however, are insulating and not responsible for the observed superconductivity. Studies by transmission electron microscopy,[3] synchrotron X-ray diffraction,[4] Mössbauer spectroscopy,[5] nuclear magnetic resonance,[6] muon spin spectroscopy,[7] scanning tunneling microscopy,[8] infrared spectroscopy,[9] and Raman spectroscopy[10] gave strong evidence that phase separations occur in $A_xFe_{2-y}Se_2$, leading to 245 phases with $\sqrt{5}\times\sqrt{5}\times1$ superstructure and coexisting superconducting (SC) phases. Changing initial compositions, heating procedures, and cooling rates did not to prevent the phase separations.[11]

SC phases are generally thought to precipitate from $A_xFe_{2-y}Se_2$ into nanoscale strips that intergrow with the 245 phases,[4] though other formation routes cannot be ruled out. Their volume fractions are low, 10−20% estimated by various techniques.[4−7] All experimental results suggest that they are isostructural to $BaFe_2As_2$[12] with Fe vacancy free and can be represented by chemical formula $A_xFe_2Se_2$.[3c,4,6,8] The deduced alkali occupancies, however, are inconsistent, varying from x = 0.3 to 1.0[4,6,8] because of the lack of single-phase samples. Previous efforts to obtain pure or SC-dominated phases by using Bridgeman or other high-temperature routes have failed. A 44 K SC phase with trace fraction was also observed apart from the 30 K phase in some samples,[11a,13] further complicating the identification of SC phases. Thus, one has good reasons to think the previously reported properties of this family of superconductors are flawed or even dubious, considering that the "single-crystal" samples on which measurements were done actually consist of majority 245 phases and minority SC phases. It is a pressing and important issue to obtain pure SC phases or real single crystals to clarify their peculiar electronic structures[14] and study the intrinsic properties of this new family of superconductors.

Previously we reported the syntheses of a series of superconductors with T_c = 30−46 K by intercalating metals Li, Na, K, Ba, Sr, Ca, Eu, and Yb between FeSe layers via an ammonothermal route,[15] which allows us to tune the concentrations of intercalated metals at room temperature, implying an alternative for preventing phase separation. Now we report that, in the K-intercalated iron selenides, there are at least two SC phases, differing mainly in potassium concentration. Both phases are Fe vacancy free and can be represented by $K_xFe_2Se_2(NH_3)_y$, with $x \approx 0.3$ corresponding to the 44 K phase and $x \approx 0.6$ to 30 K. We show that the inserted NH_3 has little, if any, effect on superconductivity. No antiferromagnetic orderings are observed

Table 1. K, Fe, and Se Nominal Compositions and Sample Compositions Including NH_3 Characterized by ICP-AES and Standard Micro-Kjeldahl Method

sample	nominal composition	composition by ICP-AES and micro-Kjeldahl method
1	$K_{0.2}Fe_2Se_2+NH_3$	$K_{0.2}Fe_{2.03}Se_2(NH_3)_{0.45}$
2	$K_{0.25}Fe_2Se_2+NH_3$	$K_{0.24}Fe_{1.98}Se_2(NH_3)_{0.49}$
3	$K_{0.27}Fe_2Se_2+NH_3$	$K_{0.26}Fe_{2.01}Se_2(NH_3)_{0.45}$
4	$K_{0.3}Fe_2Se_2+NH_3$	$K_{0.28}Fe_{1.97}Se_2(NH_3)_{0.47}$
5	$K_{0.35}$ $Fe_2Se_2+NH_3$	$K_{0.33}$ $Fe_{1.96}Se_2(NH_3)_{0.4}$
6	$K_{0.4}$ $Fe_2Se_2+NH_3$	$K_{0.4}$ $Fe_2Se_2(NH_3)_{0.5}$
7	$K_{0.45}$ $Fe_2Se_2+NH_3$	$K_{0.44}$ $Fe_{1.98}Se_2(NH_3)_{0.4}$
8	$K_{0.5}$ $Fe_2Se_2+NH_3$	$K_{0.48}$ $Fe_{2.02}Se_2(NH_3)_{0.35}$
9	$K_{0.6}$ $Fe_2Se_2+NH_3$	$K_{0.6}$ $Fe_2Se_2(NH_3)_{0.37}$
10	$K_{0.65}Fe_2Se_2+NH_3$	$K_{0.62}Fe_2Se_2(NH_3)_{0.35}$
11	$K_{0.7}$ $Fe_2Se_2+NH_3$	$K_{0.57}Fe_{2.02}Se_2(NH_3)_{0.34}$
12	$K_{0.8}$ $Fe_2Se_2+NH_3$	$K_{0.68}Fe_2Se_2(NH_3)_{0.3}$

Received: December 31, 2012
Published: February 13, 2013

ACS Publications © 2013 American Chemical Society

dx.doi.org/10.1021/ja312705x | J. Am. Chem. Soc. 2013, 135, 2951−2954

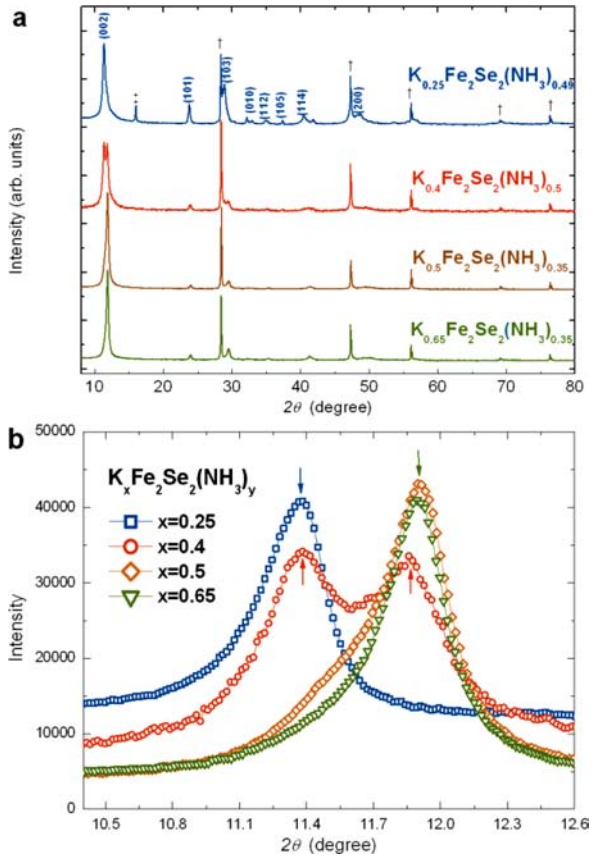

Figure 1. (a) PXRD patterns for samples with nominal compositions $K_xFe_2Se_2(NH_3)_y$ (x = 0.25, 0.4, 0.5, and 0.65, respectively) measured at 297 K with Cu Kα radiation, referenced against Si powder (NIST SRM 640, denoted with †). For x = 0.25, residual β-FeSe is observed, noted with ‡. With increasing potassium content, the lattice with larger cell constant c weakens and another lattice with smaller c develops. The coexistence of these two phases is clearly seen at x = 0.4. For x = 0.4, 0.5, and 0.65, no peaks corresponding to β-FeSe are observed. (b) Enlargement of (002) peaks, marked with arrows. Unless otherwise specified, x represents nominal compositions for clarity.

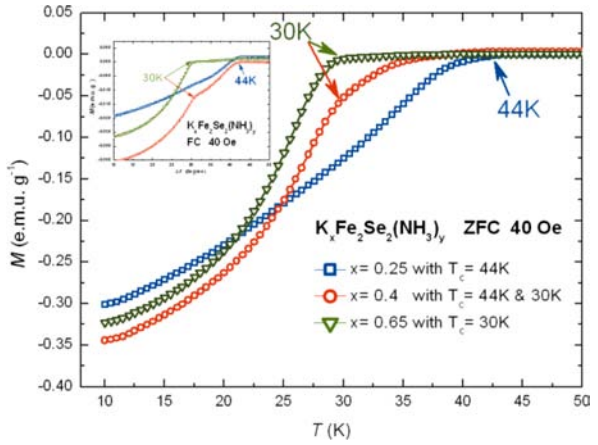

Figure 2. $M-T$ curves of samples with different nominal potassium contents under zero-field cooling. When x = 0.25 and 0.4, onset T_c = 44 K is observed. For x = 0.65, T_c shifts to 30 K. Inset: transition temperature region for the corresponding $M-T$ curves under field cooling. An inflection point at 30 K can be clearly seen for $K_{0.4}Fe_2Se_2(NH_3)_{0.5}$.

for either phase. Unlike iron pnictide superconductors, only two discrete potassium doping levels are allowed, to stabilize the structure, and the variation of T_c with doping level does not exhibit a dome-like curve, as in the cuprate and pnictide superconductors.

A series of samples $K_xFe_2Se_2(NH_3)_y$ with nominal x = 0.1, 0.2, 0.25, 0.27, 0.3, 0.35, 0.4, 0.45, 0.5, 0.6, 0.7, 0.8, and 1.0 were synthesized by a liquid NH_3 method (details are given in the Supporting Information). The key to obtain phase-pure samples is to use high-purity FeSe precursors; impurities will capture the solvated electrons first and impede potassium intercalation. Chemical analyses were done by inductively coupled plasma atomic emission spectrometry (ICP-AES) for K, Fe, and Se. Caution should be taken to avoid the escape of H_2Se during measurements, which often leads to underestimated Se contents. ICP-AES analyses indicate Fe:Se is very close to 1:1 for all thus-obtained samples within errors <2%, strongly indicating that these samples are Fe vacancy free. The potassium amounts in samples matched well with the predetermined initial amounts, with variations <7% for x < 0.6. Potassium amounts in samples remained at ~0.6 despite further increasing initial potassium amounts. We determined the NH_3 amounts in these compounds by the standard micro-Kjeldahl method (see Table 1). The NH_3 amount, y, varies in samples and is <0.5 in all cases, roughly in inverse proportion with potassium content. Phase identifications were performed on an X-ray diffractometer with Cu Kα radiation. Indexing was aided by use of a Si standard to obtain precise lattice constants. Magnetic measurements were performed on powder samples. The estimated SC volume fractions at 10 K from zero-field-cooling curves and transition temperatures (T_c) for all samples are presented in Table S1.

Figure 1a shows the powder X-ray diffraction (PXRD) patterns for nominal $K_xFe_2Se_2(NH_3)_y$ samples with x = 0.25, 0.4, 0.5, and 0.65. Peaks marked with † are from Si (Standard Reference Material, SRM640), which was added in all samples to correct the diffraction peak positions. All patterns can be indexed as a tetragonal body-centered cell with lattice constants a = 3.82–3.85 Å and c = 14.8–15.7 Å, indicating that varying amounts of potassium are intercalated between the FeSe layers. We note that (00l) diffractions are the most well-defined among all peaks due to preferred orientations; thus, they are good indicators of phase identification and variation of c with intercalated potassium. From the magnified pattern for (002) in Figure 1b, we can clearly see peak shifts with the potassium intercalations. A striking feature is that the peak shifts are not continuous with the potassium content. Instead, peaks only appear at $2\theta \approx 11.36°$ and 11.89°, corresponding to c = 15.56(1) and 14.84(1) Å in all samples, respectively. For instance, $K_{0.25}Fe_2Se_2(NH_3)_{0.49}$ exhibits one (002) peak at 2θ = 11.36°, and $K_{0.65}Fe_2Se_2(NH_3)_{0.35}$ at 2θ = 11.89°, indicating these samples consist of only one K-intercalated phase with different constants c. In contrast, $K_{0.4}Fe_2Se_2(NH_3)_{0.5}$ has two (002) peaks, meaning it contains both phases.

The magnetism of all samples was measured from room temperature to 10 K. Shown in Figure 2 are typical $M-T$ curves under zero-field cooling for $K_{0.25}Fe_2Se_2(NH_3)_{0.49}$, $K_{0.4}Fe_2Se_2(NH_3)_{0.5}$, and $K_{0.65}Fe_2Se_2(NH_3)_{0.35}$. Onset T_cs are 44, 44, and 30 K, respectively. An inflection point at 30 K can be clearly seen in the field-cooling curve for $K_{0.4}Fe_2Se_2(NH_3)_{0.5}$ (inset), implying that two SC phases coexist. While no apparent inflections are observed in $K_{0.25}Fe_2Se_2(NH_3)_{0.49}$ and $K_{0.65}Fe_2Se_2(NH_3)_{0.35}$, they can be regarded 44 and 30 K phase-dominated, respectively. In addition, inflection points at 36 K appear in some samples with $x \approx 0.35–0.55$. All data for the T_c

dx.doi.org/10.1021/ja312705x | J. Am. Chem. Soc. 2013, 135, 2951–2954

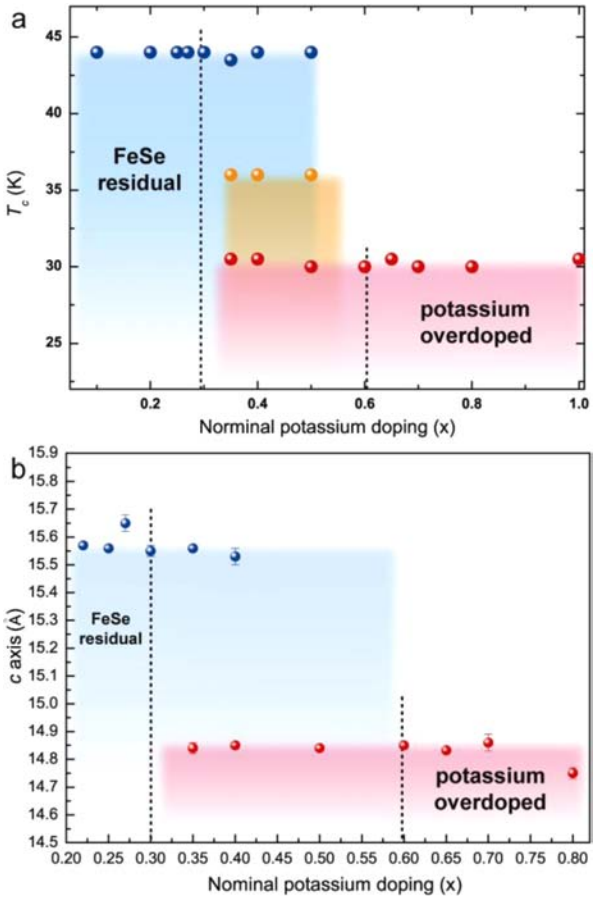

Figure 3. (a) T_cs of $K_xFe_2Se_2(NH_3)_y$ as a function of nominal potassium content. They show abrupt rather than dome-like changes with potassium content. With $x < 0.3$, there is residual β-FeSe, which could be distinguished from diffraction patterns. With $x > 0.6$, the unique blue color induced by potassium dissolved in liquid NH_3 does not fade within several minutes, and potassamide is finally obtained, adhering on the tube wall. The transition at 36 K does not exist alone but is always accompanied by a transition at 44 or 30 K. (b) Lattice constants c of $K_xFe_2Se_2(NH_3)_y$ vs nominal potassium content. Two distinct c values are displayed that coexist for x between 0.3 and 0.6.

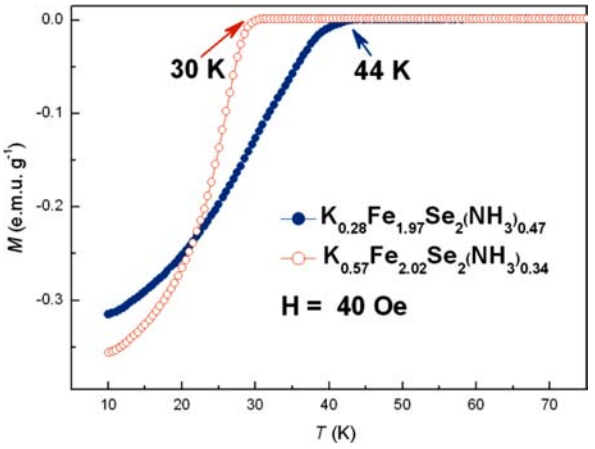

Figure 4. $M-T$ curves of $K_{0.28}Fe_{1.97}Se_2(NH_3)_{0.47}$ before and after further reaction under zero-field cooling. For $K_{0.28}Fe_{1.97}Se_2(NH_3)_{0.47}$, transition at 44 K is observed. After further reacting with potassium in liquid NH_3, $K_{0.28}Fe_{1.97}Se_2(NH_3)_{0.47}$ is converted into $K_{0.57}Fe_{2.02}Se_2(NH_3)_{0.34}$. T_c is down to 30 K. Chemical formulas in this figure are real compositions.

and c are summarized in Figure 3. With $x < 0.3$, all samples exhibit onset $T_c = 44$ K and $c = 15.56(1)$ Å, while with $x > 0.6$, all samples exhibit onset $T_c = 30$ K and $c = 14.84(1)$ Å. Between $x \approx 0.3$ and 0.6, the samples' SC transitions start at 44 K, with distinct inflection points at 36 or 30 K, indicating the samples contain two or three SC phases. Lattice constant c relating to the 36 K phase, however, is not observed; the reason is unknown at present. To verify T_c is potassium dependent, we increase the potassium doping amount by further reacting $K_{0.3}Fe_2Se_2(NH_3)_{0.47}$ with potassium in liquid NH_3. Chemical analyses confirm that the potassium concentration increases from 0.28 to 0.57, while there is almost no compositional change in Fe and Se after reaction. A dramatic change in superconductivity ensues. Figure 4 shows the $M-T$ curve for the $K_{0.3}Fe_2Se_2(NH_3)_{0.47}$ sample before and after further reaction. It can be clearly seen that the 44 K phase is converted into the 30 K phase.

These results demonstrate that there are at least two SC phases in the K-intercalated iron selenides, one close to $K_{0.3}Fe_2Se_2(NH_3)_{0.47}$ with $T_c = 44$ K and another close to $K_{0.6}Fe_2Se_2(NH_3)_{0.37}$ with $T_c = 30$ K. These two phases are isostructural to each other, except for the former phase's lattice a shrinking a little and c expanding in comparison with those of the latter. The enhanced T_c from 30 to 44 K is attributed to the decrease in intercalated potassium amount from 0.6 to 0.3, implying that the 30 K phase is overdoped by electrons. Most importantly, this study reveals a striking feature of $K_xFe_2Se_2(NH_3)_y$ superconductors: the variation of T_c vs potassium doping is not continuous but discrete, simply because the stable phases only appear at certain doping levels. This feature is unique to $K_xFe_2Se_2(NH_3)_y$, as all cuprate and pnictide superconductors show dome-like variations of T_c and continuous variations of lattice constants with doping.

Lattice constants $c = 15.56(1)$ Å for $K_{0.3}Fe_2Se_2(NH_3)_{0.47}$ and $c = 14.84(1)$ Å for $K_{0.6}Fe_2Se_2(NH_3)_{0.37}$ are much longer than $c \approx 14.2$ Å[3c,4,8] for the SC phase without NH_3, suggesting that between FeSe layers there exist other atoms or atomic groups, as we previously pointed out.[15] Using a similar method, Burrard-Lucas et al.[16] intercalated Li into FeSe layers and found that lithium amide and NH_3 exist apart from Li ion in the product compound, characterized by neutron diffractions. Scheidt et al.[17] ruled out the existence of lithium amide between FeSe layers on the basis of their own experiments. To study the effects of NH_3 on structure and superconductivity, we extracted NH_3 while avoiding the collapse of the lattice and found that the optimal extraction temperature is ~200 °C. As-prepared $K_{0.3}Fe_2Se_2(NH_3)_{0.47}$, sealed in a tube, was first placed in an oil bath while slowly heating to 200 °C, and then evacuated for several hours. The PXRD pattern (see Figure S1) shows that the tetragonal body-centered phase remains while a expands from 3.843(1) to 3.87(1) Å and c shrinks a lot from 15.56(1) to 14.28(4) Å after the heating process. This c value is very close to that reported for the SC phase obtained by high-temperature routes.[3c,4,8] The temperature-dependent magnetization in Figure S2 shows the onset T_c is still close to 44 K. A similar situation is found in $K_{0.6}Fe_2Se_2(NH_3)_{0.37}$. These results demonstrate that NH_3 has little, if any, influence on T_c. Although our results are based on NH_3-containing samples, the conclusions should apply to $K_{0.3}Fe_2Se_2$ and $K_{0.6}Fe_2Se_2$ SC phases, although NH_3 causes changes in the lattice constants.

Recently, Yan and Miao[18] pointed out, based on first-principles calculations, that the 40 and 30 K phases in KFe_2Se_2 are due to different occupying sites of potassium in the $I4/mmm$

dx.doi.org/10.1021/ja312705x | J. Am. Chem. Soc. 2013, 135, 2951−2954

lattice, leading to c = 18.6−19.04 and 15.46−16.7 Å, respectively. Our results do not support their calculations, as the amount of intercalated potassium at the body-centered site plays a crucial role in determining the SC phases. The elongated lattice constants c are attributed to inserted NH_3,[15−17] as with other inserted atomic groups.[19] Inserted NH_3 is very likely to form a H-bond, and its position is restricted by the trigonal pyramidal shape. A very tentative structure model has the NH_3 arranged to occupy the space between FeSe layers along with potassium, leading to the expansion of the constant c. NH_3 can be extracted, causing the constant c to decrease, as we demonstrated above.

Last, we point out that all these SC phases are paramagnetic above T_c, in agreement with recently reported results.[7] Figure S3 shows the magnetization vs temperature from 10 to 400 K under a field of 1 T for $K_{0.27}Fe_2Se_2(NH_3)_{0.45}$. The magnetization value and its trend vs temperature reveal that the sample contains no Fe vacancy phases, such as 245 phase or Fe_7Se_8, agreeing well with the findings of our chemical analyses that the obtained SC phases are Fe vacancy free.

In summary, in the K-intercalated iron selenides, there exist at least two superconducting phases with $ThCr_2Si_2$ structure type. Both have vacancy-free FeSe layers, but different potassium concentrations. It is the potassium concentration that determines the SC transition temperatures. $K_{0.3}Fe_2Se_2(NH_3)_{0.47}$ and $K_{0.6}Fe_2Se_2(NH_3)_{0.37}$ stand out among known superconductors in that their structures are stable only at certain potassium doping levels, and hence the variation of T_c with doping is not dome-like. The mechanism behind these unique properties needs further investigation to be understood.

■ ASSOCIATED CONTENT

Ⓢ Supporting Information

Experimental details and analyses. This material is available free of charge via the Internet at http://pubs.acs.org.

■ AUTHOR INFORMATION

Corresponding Author

chenx29@iphy.ac.cn; gangwang@iphy.ac.cn

Notes

The authors declare no competing financial interest.

■ ACKNOWLEDGMENTS

T.Y. thanks P. Zheng and Y. G. Shi from Institute of Physics, CAS, for help with magnetic measurements. This work was partly supported by the National Natural Science Foundation of China under Grant Nos. 90922037, 51072226, and 51202286, the Chinese Academy of Sciences, and the ICDD.

■ REFERENCES

(1) (a) Guo, J. G.; Jin, S. F.; Wang, G.; Wang, S. C.; Zhu, K. X.; Zhou, T. T.; He, M.; Chen, X. L. *Phys. Rev. B* **2010**, *82*, 180520. (b) Krzton-Maziopa, A.; Shermadini, Z.; Pomjakushina, E.; Pomjakushin, V.; Bendele, M.; Amato, A.; Khasanov, R.; Luetkens, H.; Conder, K. *J. Phys.: Condens. Matter* **2011**, *23*, 052203. (c) Wang, A. F.; Ying, J. J.; Yan, Y. J.; Liu, R. H.; Luo, X. G.; Li, Z. Y.; Wang, X. F.; Zhang, M.; Ye, G. J.; Cheng, P.; Xiang, Z. J.; Chen, X. H. *Phys. Rev. B* **2011**, *83*, 060512. (d) Wang, H.-D.; Dong, C.-H.; Li, Z.-J.; Mao, Q.-H.; Zhu, S.-S.; Feng, C.-M.; Yuan, H. Q.; Fang, M.-H. *Europhys. Lett.* **2011**, *93*, 47004. (e) Fang, M.-H.; Wang, H.-D.; Dong, C.-H.; Li, Z.-J.; Feng, C.-M.; Chen, J.; Yuan, H. Q. *Europhys. Lett.* **2011**, *94*, 27009. (f) Wen, H. H. *Rep. Prog. Phys.* **2012**, *75*, 112501. (g) Dagotto, E. *arXiv* **2012**, *1210*, 6501.

(2) (a) Ye, F.; Chi, S.; Bao, W.; Wang, X. F.; Ying, J. J.; Chen, X. H.; Wang, H. D.; Dong, C. H.; Fang, M. *Phys. Rev. Lett.* **2011**, *107*, 137003. (b) Liu, R. H.; Luo, X. G.; Zhang, M.; Wang, A. F.; Ying, J. J.; Wang, X. F.; Yan, Y. J.; Xiang, Z. J.; Cheng, P.; Ye, G. J.; Li, Z. Y.; Chen, X. H. *Europhys. Lett.* **2011**, *94*, 27008. (c) Pomjakushin, V. Y.; Pomjakushina, E. V.; Krzton-Maziopa, A.; Conder, K.; Shermadini, Z. *J. Phys.: Condens. Matter* **2011**, *23*, 156003. (d) Shermadini, Z.; Krzton-Maziopa, A.; Bendele, M.; Khasanov, R.; Luetkens, H.; Conder, K.; Pomjakushina, E.; Weyeneth, S.; Pomjakushin, V.; Bossen, O.; Amato, A. *Phys. Rev. Lett.* **2011**, *106*, 117602. (e) Bao, W.; Huang, Q.-Z.; Chen, G. F.; Green, M. A.; Wang, D.-M.; He, J.-B.; Qiu, Y.-M. *Chin. Phys. Lett.* **2011**, *28*, 086104.

(3) (a) Wang, Z.; Song, Y. J.; Shi, H. L.; Wang, Z. W.; Chen, Z.; Tian, H. F.; Chen, G. F.; Guo, J. G.; Yang, H. X.; Li, J. Q. *Phys. Rev. B* **2011**, *83*, 140505. (b) Chen, F.; Xu, M.; Ge, Q. Q.; Zhang, Y.; Ye, Z. R.; Yang, L. X.; Jiang, J.; Xie, B. P.; Che, R. C.; Zhang, M.; Wang, A. F.; Chen, X. H.; Shen, D. W.; Hu, J. P.; Feng, D. L. *Phys. Rev. X* **2011**, *1*, 021020. (c) Wang, Z.-W.; Wang, Z.; Song, Y.-J.; Ma, C.; Cai, Y.; Chen, Z.; Tian, H.-F.; Yang, H.-X.; Chen, G.-F.; Li, J.-Q. *J. Phys. Chem. C* **2012**, *116*, 17847.

(4) Shoemaker, D. P.; Chung, D. Y.; Claus, H.; Francisco, M. C.; Avci, S.; Llobet, A.; Kanatzidis, M. G. *Phys. Rev. B* **2012**, *86*, 184511.

(5) Ksenofontov, V.; Wortmann, G.; Medvedev, S. A.; Tsurkan, V.; Deisenhofer, J.; Loidl, A.; Felser, C. *Phys. Rev. B* **2011**, *84*, 180508.

(6) Texier, Y.; Deisenhofer, J.; Tsurkan, V.; Loidl, A.; Inosov, D. S.; Friemel, G.; Bobroff, J. *Phys. Rev. Lett.* **2012**, *108*, 237002.

(7) Shermadini, Z.; Krzton-Maziopa, A.; Bendele, M.; Khasanov, R.; Luetkens, H.; Conder, K.; Pomjakushina, E.; Weyeneth, S.; Pomjakushin, V.; Bossen, O.; Amato, A. *Phys. Rev. Lett.* **2011**, *106*, 117602.

(8) Li, W.; Ding, H.; Deng, P.; Chang, K.; Song, C.; He, K.; Wang, L.; Ma, X.; Hu, J.-P.; Chen, X.; Xue, Q.-K. *Nat. Phys.* **2012**, *8*, 126.

(9) Yuan, R. H.; Dong, T.; Song, Y. J.; Zheng, P.; Chen, G. F.; Hu, J. P.; Li, J. Q.; Wang, N. L. *Sci. Rep.* **2012**, *2*, 221.

(10) Zhang, A. M.; Xiao, J. H.; Li, Y. S.; He, J. B.; Wang, D. M.; Chen, G. F.; Normand, B.; Zhang, Q. M.; Xiang, T. *Phys. Rev. B* **2012**, *85*, 214508.

(11) (a) Wang, D. M.; He, J. B.; Xia, T.-L.; Chen, G. F. *Phys. Rev. B* **2011**, *83*, 132502. (b) Weyeneth, S.; Bendele, M.; von Rohr, F.; Dluzewski, P.; Puzniak, R.; Krzton-Maziopa, A.; Bosma, S.; Guguchia, Z.; Khasanov, R.; Shermadini, Z.; Amato, A.; Pomjakushina, E.; Conder, K.; Schilling, A.; Keller, H. *Phys. Rev. B* **2012**, *86*, 134530. (c) Liu, Y.; Xing, Q.; Dennis, K. W.; McCallum, R. W.; Lograsso, T. A. *Phys. Rev. B* **2012**, *86*, 144507.

(12) Rotter, M.; Tegel, M.; Johrendt, D. *Phys. Rev. Lett.* **2008**, *101*, 107006.

(13) Zhang, A. M.; Xia, T.-L.; Liu, K.; Tong, W.; Yang, Z. R.; Zhang, Q. M. *Sci. Rep.* **2013**, *3*, 1216.

(14) (a) Qian, T.; Wang, X. P.; Jin, W.-C.; Zhang, P.; Richard, P.; Xu, G.; Dai, X.; Fang, Z.; Guo, J.-G.; Chen, X.-L.; Ding, H. *Phys. Rev. Lett.* **2011**, *106*, 187001. (b) Zhang, Y.; Yang, L. X.; Xu, M.; Ye, Z. R.; Chen, F.; He, C.; Xu, H. C.; Jiang, J.; Xie, B. P.; Ying, J. J.; Wang, X. F.; Chen, X. H.; Hu, J. P.; Matsunami, M.; Kimura, S.; Feng, D. L. *Nat. Mater.* **2011**, *10*, 273. (c) Mou, D.; Liu, S.; Jia, X.; He, J.; Peng, Y.; Zhao, L.; Yu, L.; Liu, G.; He, S.; Dong, X.; Zhang, J.; Wang, H.; Dong, C.; Fang, M.; Wang, X.; Peng, Q.; Wang, Z.; Zhang, S.; Yang, F.; Xu, Z.; Chen, C.; Zhou, X. J. *Phys. Rev. Lett.* **2011**, *106*, 107001. (d) Zhao, L.; Mou, D.; Liu, S.; Jia, X.; He, J.; Peng, Y.; Yu, L.; Liu, X.; Liu, G.; He, S.; Dong, X.; Zhang, J.; He, J. B.; Wang, D. M.; Chen, G. F.; Guo, J. G.; Chen, X. L.; Wang, X.; Peng, Q.; Wang, Z.; Zhang, S.; Yang, F.; Xu, Z.; Chen, C.; Zhou, X. J. *Phys. Rev. B* **2011**, *83*, 140508.

(15) Ying, T. P.; Chen, X. L.; Wang, G.; Jin, S. F.; Zhou, T. T.; Lai, X. F.; Zhang, H.; Wang, W. Y. *Sci. Rep.* **2012**, *2*, 426.

(16) Burrard-Lucas, M.; Free, D. G.; Sedlmaier, S. J.; Wright, J. D.; Cassidy, S. J.; Hara, Y.; Corkett, A. J.; Lancaster, T.; Baker, P. J.; Blundell, S. J.; Clarke, S. J. *Nat. Mater.* **2013**, *12*, 15.

(17) Scheidt, E.-W.; Hathwar, V. R.; Schmitz, D.; Dunbar, A.; Scherer, W.; Mayr, F.; Tsurkan, V.; Deisenhofer, J.; Loidl, A. *Eur. Phys. J. B* **2012**, *85*, 279.

(18) Yan, X.-W.; Gao, M. J. *Phys.: Condens. Matter* **2012**, *24*, 455702.

(19) Krzton-Maziopa, A.; Pomjakushina, E. V.; Pomjakushin, V. Y.; von Rohr, F.; Schilling, A.; Conder, K. *J. Phys.: Condens. Matter* **2012**, *24*, 382202.